

Spatiotemporal Monitoring of Electricity Consumption by Using Residual-based Control Charts

MINA KHAZAIE POUL¹, HIWA FARUGHI^{1,*}, AND YASER SAMIMI²

¹Department of Industrial Engineering, Faculty of Engineering, University of Kurdistan, Sanandaj, Iran

²Department of Industrial Engineering, K. N. Toosi University of Technology, Tehran, Iran

*Corresponding author email: h.farughi@uok.ac.ir

Manuscript received 02 February, 2023; revised 07 June, 2023; accepted 30 June, 2023. Paper no. JEMT-2304-1431.

The optimum use of energy carriers is one of the important factors affecting the sustainable growth and development of countries. Therefore, monitoring energy consumption is of considerable importance. Energy monitoring with Statistical Process Control (SPC) methods provides a breakdown of energy usage and makes it easier to perceive trends to reduce consumption. A review of the literature shows that previous research has addressed detecting change's time in consumption. Developing these methods in spatial and temporal aspects of changes in energy consumption, which means detecting the time and location of changes simultaneously, would be able to provide more accurate diagnostic information. In this paper, a novel spatiotemporal framework based on the extension of the generalized likelihood ratio (GLR) and T2 control charts are used for monitoring the electricity consumption of eight-time series related to eight western cities in Mazandaran province, North of Iran, from March 21, 2019, to August 21, 2019. Due to the presence of autocorrelation in electricity consumption data, a model-based approach is proposed to reduce the autocorrelation's effect on chart performance. The performance of the proposed charts in identifying significant deviations in electricity consumption was evaluated, which indicates the greater diagnostic power of the GLR chart in detecting the time and location of changes. Application of the recently-established spatiotemporal surveillance mechanisms for energy consumption monitoring is the main contribution of this study it would enable practitioners to analyze discrepancies of usage patterns better and make policies for continual improvement of the regional management of electricity distribution.

© 2023 Journal of Energy Management and Technology

keywords: Electricity Consumption, Spatiotemporal Monitoring, Statistical Process Control, Residual-based Control Chart, Autocorrelation.

<http://dx.doi.org/10.22109/JEMT.2023.384070.1431>

NOMENCLATURE

Abbreviation

ARL	Average run length
ARMA	Autoregressive moving-average
ACF	Autocorrelation function
CUSUM	Cumulative sum
EWMA	Exponentially Weighted Moving Average
GLR	Generalized likelihood ratio
MCUSUM	Lower Control Limit

MEWMA Multivariate Exponentially Weighted moving average

MLE Maximum likelihood estimator

PACF Partial autocorrelation function

SPC Statistical process control

UCL Upper Control Limit

INDEX

i, j Index of regions

K Number of sample

L	Temporal lag operator
M	Number of observation
N	Number of observation
p	Order of autoregressive model
q	Order of moving average model
t	Index of time
τ	Shift time
h_{GLR}	Control limit of GLR
S_{xx}	$(p-1) \times (p-1)$ Sub matrix of s
$T_{p 1,2,\dots,p-1}^2$	Approximation of individual observations in Phase I
W	Spatial weight matrix
x_i, x_j	Observed value
X_i	Sample vector
\bar{X}	Sample mean vector
$X_i^{(p-1)}$	Mean vector of the first p-1 variable
Y_t	Observed value
μ_0	Mean vector before shift time
μ_1	Mean vector after shift time
Σ_0	Covariance matrix

1. INTRODUCTION

Energy has the largest share of world trade and has a special place in all human activities. Due to the high energy consumption per capita and the increasing limitations in accessing energy resources, energy consumption management is of considerable importance. Energy management is systematic monitoring, optimization and control of energy consumption to save energy and reduce energy costs. Energy monitoring is a chain of related concepts, including forecasting, modeling, controlling and analyzing energy consumption which can be investigated by various techniques such as designing measurement devices, introducing software, using statistical process control (SPC) tools, etc., with the aim of optimizing consumption and providing accurate information for management decisions at micro and macro levels. Some studies in this field are to be discussed below and briefly shown in Table 1.

Rizzo et al. extended an autonomous system for monitoring water consumption in smart houses which used turbine flow sensors and ZigBee technology to send consumption volume to users [1]. Hameed and Barnouti developed an Internet of Things intelligent (IoT) device for tracking energy consumption, monitoring the time in which a generator operates and calculating how much fuel is used. Finally, some suggestions on how to avoid waste of resources have been outlined through an analysis of the collected data using Apriori decision making algorithm [2]. In order to predict electricity demand at an Italian healthcare facility, Zini and Carcasci have developed a monitoring approach based on machine learning which takes into account the correlation of weather conditions, time and health activities [3]. Melendez et al. have developed a web service module for tracking the energy consumption of buildings, using the Multivariate Principal Component Analysis (MPCA). To identify these unexpected energy use patterns, two control charts, including T2 and Q, have been applied [4]. Stuart et al. based on

half-hourly electricity consumption data, proposed a methodology to find opportunities for electricity saving in school buildings in the United Kingdom [5]. The method involves using a cumulative sum (CUSUM) control chart for monitoring time series data and identifying temporal changes in consumption. To monitoring energy consumption in the melting furnaces of a foundry, Puranik used the CUSUM chart to identify abnormal changes in the process quickly [6]. Braga et al. used a multi-channel structure for modeling and estimating the building's energy consumption profile during a predetermined cycle, and then applied CUSUM chart for monitoring and detecting any unusual behavior in energy demand [7]. Shamsuzzaman et al. demonstrated the design and application of an economical \bar{X} control chart based on Duncan's model to monitor and identify anomalous power loss in the transmission and distribution systems [8]. In another study Shamsuzzaman et al., proposed the combined \bar{X} & Exponentially Weighted Moving Average (EWMA) scheme for monitoring the carbon emissions of industrial facilities and comparing the performance of the proposed scheme with a basic chart including \bar{X} , EWMA, and a basic \bar{X} & EWMA, which showed its better performance in reducing the expected total cost [9]. Houidi et al. focused on detecting changes in Home Electrical Appliances in a Non-Intrusive Load Monitoring context by extending some excited change detector algorithms, including Bayesian Information Criterion (BIC), the CUSUM, and the Hotelling T^2 test, in the multidimensional case [10]. Faisal et al, proposed a modified CUSUM chart based on a link relative variable transformation technique to increase its sensitivity for detecting small and moderate shifts. Average run length (ARL) was considered to evaluate its performance with a conventional chart, which indicated the overall good detection of the proposed scheme. A real-world example from the electrical engineering process was considered as an application of the proposed chart [11]. Golmohammadi and Golestan, focused on investigating energy consumption monitoring in an Iranian cement factory. They considered the clinker production process, which consumed more than 90% of the total energy consumption, and used I-MR control chart to detected significant shifts in the process [12].

As seen in the literature review, using SPC tools for monitoring energy has been investigated from different aspects to control and improve consumption. So SPC tools can be used successfully to continuously monitor the consumption data and identify unusual changes on time. Control charts are one of the most common process control tools used for monitoring the qualitative characteristics of the process, identifying shifts in the process, and finding assignable causes of variation [13]. The advantage of using control charts is in identifying any changes in the pattern of consumption and then taking corrective actions by using accurate information about the causes of the change and the pattern of change in consumption to return the process to in-controlled state. This can be applied like a PDCA cycle throughout the life of the process. SPC techniques, including control charts, are widely used in the manufacturing industry for monitoring qualitative characteristics of processes, their application to the energy sector presents unique challenges. One of the main limitations is related to the availability and standardization of energy consumption data. Unlike the manufacturing sector, where the quality characteristics of a product can be easily defined and measured, energy consumption data may be more difficult to access and standardize. This poses challenges in selecting the appropriate control chart and identifying the distribution of the data, testing the stationary of time series, and

Table 1. Overview of the reviewed studies

Reference	Purpose	Technique/method used	Application
[5]	Monitoring energy consumption and identifying its changes	SPC/ CUSUM chart	School buildings in the United Kingdom
[6]	Monitoring energy use performance	SPC/ CUSUM chart	Melting furnaces of the foundry industry
[7]	Monitoring, assessing and tracking energy consumption	SPC/ CUSUM chart	An educational complex of a Brazilian University
[4]	Monitoring buildings energy consumption and detecting anomalies in consumption	A web service module based on MPCA and using T2 and Q charts	A large office building in France
[11]	Monitoring industrial processes	Modified CUSUM based on a link relative variable transformation technique	Electrical engineering process
[12]	Monitoring Energy Consumption	SPC/ I-MR chart	The clinker production process in an Iranian cement factory
[2]	Monitoring and controlling energy consumption and working time of the generator and calculating the amount of consumed fuel	An effective IoT smart device	An electricity generator
[10]	Non-Intrusive Load Monitoring for analyzing electrical signals of Home Electrical Appliances	BIC, the CUSUM, the Hotelling T2 test	Residential buildings
[8]	Monitoring and identifying anomalous power loss in the transmission and distribution systems	SPC/ \bar{X} Chart	Electricity consumption of subscribers
[9]	Monitoring carbon emissions	SPC combined \bar{X} & EWMA	Industrial sector
[1]	Monitoring water consumption	Building an autonomous water meter	Smart houses
[3]	Monitoring and analyzing electricity consumption	Machine Learning method	A healthcare facility in Italy

ensuring the independence of observations.

The focus of energy monitoring studies using control charts is identifying temporal change in consumption, while the nature of energy data will be affected by various factors such as geographical location, climatic conditions, population dispersion, etc., so considering the spatial dimension of data, which enables decision makers to manage the trend of consumption changes better, can be useful for monitoring energy consumption.

Recently many researchers have focused on spatiotemporal monitoring methods which have good performance in the rapid detection of defects in a process with sequential spatial data. Using spatiotemporal methods allows for the identification of both the spatial location of a defect and the time change at which the process shift has occurred. Some of this method's application is in detecting the occurrence of production faults, monitoring disease spread, and monitoring network system. Jiang et al proposed an MCUSUM method based on regression-adjusted clusters for spatiotemporal monitoring in a public health application to quickly detect any changes in disease incidence rates and take necessary actions for improving that [14]. To monitoring network system, Wang et al. proposed spatiotemporal control schemes based on the Multivariate Spatiotemporal Autoregressive model [15]. Derenski et al., Presented a methodology for spatial and temporal analysis of electricity and gas consumption in public schools in Los Angeles County. They investigated consumption trends by considering structural characteristics such as types (elementary, middle, and high), size, age and environmental factors. Results showed that correlations between electricity and gas consumption are time dependent [16]. Megahed et al., proposed a spatiotemporal approach based on a generalized likelihood ratio chart for monitoring image data to detect change time and change location in grayscale images of manufactured tiles. In their work, an image is divided into some partially overlapping regions, and average pixel intensities of them were monitored [17]. He et al., extended the spatiotemporal approach by using a multivariate generalized likelihood ratio chart for multiple change detection problems [18]. Koosha et al. extracted features from image data using a nonparametric regression method based on wavelet transform, and utilized a generalized likelihood ratio control chart for detecting simultaneously change point and fault location [19]. Zuo et al., proposed an EWMA and region growing for monitoring grayscale images of industrial products [20]. Colosimo and Grasso, presented a spatiotemporal method based on the spatially weighted Principal Component Analysis (ST-PCA) for monitoring video image data to quickly detect the time and the location of defects during the process. Their method was applied for detecting defects in metal additive manufacturing processes [21].

The usual structures of control charts are based on the assumption that the generated data of the process is independent of normal distribution [13]. Unfortunately, in the real world, some of these assumptions are ignored, which can lead to a decline in the performance of the control chart. An important but frequently overlooked assumption of SPC charts is the independence of observations, which means observations have autocorrelation. Noorossana and Vaghefi show that the average run length of control charts is affected when the independence assumption is violated and makes them invalid [22]. Furthermore, a process with serially correlated data may signal inaccurately and make control charts less effective. Different procedures have been proposed by researchers for monitoring autocorrelated processes. The use of residual-based control charts which are a natural extension of conventional statistical process con-

trol charts is the most popular method. For example, Sheu et al. extended the EWMA control chart for monitoring a process with autocorrelation in which a first-order autoregressive process is fitted to observation [23]. Khusna et al. proposed a residual-based maximum MCUSUM chart for autocorrelated process [24]. Žmuk applied three types of residual-based control charts, including I-chart, EWMA, and CUSUM for monitoring the performance of short-term stock. The result showed a better performance of the residual-based CUSUM chart for accessing the highest portfolio profits [25].

A literature review on energy consumption monitoring using SPC techniques shows that in most cases, researchers use univariate statistical control methods, especially univariate control charts. While the relationship of energy consumption in different geographical areas indicates a spatial correlation of observations. Therefore, using multivariate control charts for monitoring energy consumption in different regions (countries, provinces, cities, etc.) simultaneously is recommended. Furthermore, previous research for monitoring energy consumption has focused on detecting the time of changes, whereas extending these methods to include both spatial and temporal aspects of energy consumption, can obtain more precise diagnostic information.

The aim of this paper is energy consumption monitoring by a novel spatiotemporal framework based on the extension of the GLR and T2 control charts by considering the autocorrelation of consumption data. So the application of the recently-established spatiotemporal surveillance mechanisms for energy consumption monitoring is the main contribution of this study and would enable practitioners to better analyze discrepancies of usage patterns and make policies for continual improvement of the regional management.

According to the published reports of the Statistics Center of Iran, 32% of the total electricity consumption is related to the household sector. Therefore, monitoring household electricity consumption is essential. So this paper present a case study of household electricity consumption in eight-time series related to eight western cities in Mazandaran province, North of Iran, from March 21, 2019, to August 21, 2019.

The remain of content is arranged as follows: In Section 2, monitoring autocorrelated data based on the residual-based control chart and also the multivariate T^2 and GLR residual control charts are described. In Section 3, in a real-world case study, the electricity consumption of eight western cities in Mazandaran province is considered and the results of spatiotemporal monitoring of multivariate T^2 and GLR residual control charts along with a comparative assessment of proposed charts with one of the conventional chart used for monitoring energy, are presented. In section 4, the performance of charts are evaluated and finally, concluding remarks and conclusions are discussed in section 5.

2. RESIDUAL-BASED CONTROL CHART

As previously mentioned, the performance of statistical process control charts is significantly affected by the presence of autocorrelation in time series data, so using the appropriate method for monitoring this data is of importance.

In general, there are two main approaches for dealing with autocorrelation between observations at different points in a time series and controlling autocorrelation processes, including a model-based approach and a model-free approach [26]. In the model-free approach, instead of using the original autocor-

related data, the average of the data sets is used. Because this leads to the approximate independence of observations and the loss of autocorrelation, in the model-based approach, by fitting an appropriate time series model based on the autocorrelation structure of observations, the autocorrelation of observations will be eliminated and the residuals of the model will be obtained, which are expected to be uncorrelated. Then by using a residual-based control chart, the independent residuals are monitored. The method's details are described below.

Autoregressive moving-average (ARMA) models include a strong class of static time series models which are effectively used for modeling a variety of autocorrelated processes. In this model, the future value of a linear functional variable is considered from a number of previous observations and random errors. An autoregressive-moving average model of order (p, q) is defined by

$$ARMA(p, q): \Phi(L)Y_t = \theta(L)\varepsilon_t \quad (1)$$

Where Y_t is the observed value in time t , ε_t is an uncorrelated innovation process in time t ; $\Phi(L) = (1 - \Phi_1L - \Phi_2L^2 - \dots - \Phi_pL^p)$ is the autoregressive process; $\theta(L) = (1 - \theta_1L - \theta_2L^2 - \dots - \theta_qL^q)$ is the moving average process and L is the temporal lag operator.

One of the necessary conditions for using ARMA models is the stability of the time series. ARMA models have been developed to be used even when time series are unstable. In this situation, by differencing the time series of order d (minimum number of differences), it converts to the stationary model denoted by ARIMA (p, d, q) .

Box and Jenkins [27] used a three-step method to model an appropriate autocorrelation process. Their method includes providing an experimental model by analyzing historical data, estimating unknown parameters of the model, and finally evaluating the suitability of the model. They proposed using the autocorrelation function (ACF) and the partial autocorrelation function (PACF) as basic tools for identifying the orders of AR and MA terms in an ARIMA model. After determining the experimental time series model, its parameters are estimated using the least-squares method, and then the value of each observation is predicted using the previous observations. By differencing the actual and the prediction values, the residuals will be obtained. If the fitted ARIMA model has the necessary qualifications, the residuals will be independent and identically distributed (i.i.d) with a mean of zero and a standard deviation of σ^2 . In this way, control charts can be easily used for the residuals. But if the residuals aren't i.i.d, it is necessary to fit a more appropriate model, so the Box-Jenkins methodology should be iterated. To become more familiar with the approach of using time series models and monitoring the residuals with control charts, Noorossana and Saghaei [28] showed the flowchart of this methodology in Figure 1.

In the following subsections, the structures of the multivariate T2 and GLR residual control charts are briefly discussed. In examining energy consumption with location-based data, analyzing the spatial autocorrelation of regions is of special importance. Tobler's first law of geography is described by spatial autocorrelation: "Everything is related to everything else, but nearby things are more related than distant things" [29]. Spatial autocorrelation analyzes whether an observed value of a variable in one region affects the same variable in the adjacent regions or not. If this effect is positive and the increase of one variable in a region causes the increase of the same variable in the neighboring regions, this type of correlation is called positive

spatial autocorrelation, and if the existence of the variable has a negative effect on the same variable in neighboring areas, this type of autocorrelation is called negative spatial autocorrelation. If there is no special relationship between the variables in adjacent areas, it is said that there is no spatial autocorrelation. The Moran's I is a common test for measuring spatial autocorrelation developed by Patrick Alfred Pierce Moran [30], which is defined as

$$\begin{aligned} \text{Moran's } I &= \frac{\sum_{i=1}^n \sum_{j=1}^n W_{ij} C_{ij}}{S^2 \sum_{i=1}^n \sum_{j=1}^n W_{ij}} \\ &= \frac{\sum_{i=1}^n \sum_{j=1}^n W_{ij} (x_i - \bar{x})(x_j - \bar{x})}{S^2 \sum_{i=1}^n \sum_{j=1}^n W_{ij}} \end{aligned} \quad (2)$$

Where, X_i, X_j are the observed values of regions i, j and n is the number of regions, $S^2 = \frac{\sum_{i=1}^n (x_i - \bar{x})^2}{n}$ and W is the spatial weight matrix that is defined based on adjacent neighbors. Under the null hypothesis of no spatial autocorrelation, the expected value of Moran's I is $E(I) = \frac{-1}{N-1}$. Moran's I values typically range from -1 to +1. When its value is close to 1 and significantly greater than $E(I)$, indicates positive spatial autocorrelation; when it is close to -1 and less than $E(I)$, it indicates negative spatial autocorrelation, and when the value near 0 indicates no such autocorrelation

A. The Hotelling T^2 Residual Control Chart

The most common multivariate quality control chart is the Hotelling T2 chart, introduced by Harold Hotelling in 1947 [31]. The T2 control chart can find shifts in the process mean when two or more related variables are being evaluated simultaneously. This chart is especially popular in multivariate control charts compared with the multivariate moving average control (MEWMA) chart and the multivariate cumulative sum control (MCUSUM) chart due to its simplicity of understanding. Also, because of its similarity to the univariate Shewhart Control Chart, in the presence of autocorrelation, this chart is transformed into the T2 residual chart to account for the correlation that affects the process.

Let $X_i = (x_{1i}, x_{2i}, \dots, x_{ni})'$ $i = 1, 2, 3, \dots, n$, It be an observation from a normal p -variate distribution with an unknown mean vector and covariance matrix. There are two basic versions of the hotelling T^2 chart: one for subgrouped data and one for individual observations; for more details, see [13]. In this study, we are concerned with individual observations, and the T^2 statistic for each individual observation is as follows:

$$T_i^2 = (X_i - \bar{X})' S^{-1} (X_i - \bar{X}) \quad (3)$$

Where \bar{X} the sample's mean vector, and S is the sample covariance matrix. Also, the UCL in phase 1 is calculated as below:

$$UCL = \frac{(m-1)^2}{m} \beta_{\alpha, p/2, (q-p-1)/2} \quad (4)$$

where $q = (2(m-1)^2)/(3m-4)$. If, $T_i^2 > UCL$ the chart signals at the time i , and i th observation are considered as an out-of-control point.

As the estimation of the covariance matrix for individual observations is a significant issue, Holmes and Mergen [32] suggested the estimation of the variance-covariance matrix by using the difference between consecutive pairs of observations, which is defined as, $S = \frac{V'V}{2(m-1)}$ where $v_i = x_{i+1} - x_i$ for $i=1, 2, \dots, m-1$ and V is a transpose matrix of $m-1$ difference vec-

tors as $\begin{bmatrix} v_1 \\ v_2 \\ \vdots \\ v_{m-1} \end{bmatrix}$ In spite of the popularity and easily of the

$T^{\wedge 2}$ chart, interpreting its out-of-control signals may be a problem. The main disadvantage of this chart is in determining the deviated quality characteristics. In this regard, Mason et al. [33] proposed the $T^{\wedge 2}$ decomposition method. This method decomposes the $T^{\wedge 2}$ statistic into independent components, each representing the contribution of an individual variable, as follows:

$$T^{\wedge 2} = T_{p-1}^2 + T_{p|1, 2, \dots, p-1}^2 \quad (5)$$

In which the term T_{p-1}^2 refers to the first p-1 variable of T2 statistic and

$$T_{p-1}^2 = \left(X_i^{(p-1)} - X_i^{-(p-1)} \right)' S_{xx}^{-1} \left(X_i^{(p-1)} - X_i^{-(p-1)} \right) \quad (6)$$

Where $X_i^{(p-1)}$ is the mean vector of the first p-1 variable, S_{xx} is $(p-1) \times (p-1)$ a submatrix of S, and $T_{p|1, 2, \dots, p-1}^2$ is an approximation of individual observations in Phase I which is computed based on $\frac{(m-1)^2}{m} \beta_{\frac{1}{2}, \frac{m-2}{2}}$.

B. The GLR residual Control Chart

Using GLR charts, which are based on sequential likelihood-ratio tests, is an attractive and convenient way to identify a wide range of significant changes. It has been shown that these charts are very attractive from both practical and theoretical points of view. In the presence of autocorrelation, this chart is transformed into the GLR residual chart to account for the correlation that affects the process.

Let X be an observation from a p-variate normal distribution with a mean vector μ_0 and a covariance matrix Σ_0 when the process is under control. Assume that μ_0 and Σ_0 have been estimated from the samples of phase I. In this research, only changes in the mean vector are considered, which means when $\mu_0 \neq \mu_1$ whereas Σ_0 remains constant, it is assumed that the process is out-of-control. We consider the situation where the sample size is equal to 1, which means only one observation is measured in each time interval. So, the kth sample is considered as $X_k = (x_{1k}, x_{2k}, x_{3k}, \dots, x_{pk})'$

Assuming that an assignable cause occurs in the process at an unknown time τ , causing a shift in the mean of quality characteristics of subsequent samples. Up to the kth sample, there is a series of samples (X_1, X_2, \dots, X_k) , and the likelihood function for sample k would be as follows:

$$L_{\theta, k}(\mu_0, \mu_1) = \prod_{i=1}^{\theta} f(X_i | \mu_0, \Sigma_0) \times \prod_{i=\theta+1}^k f(X_i | \mu_1, \Sigma_0) \quad (7)$$

Where μ_0, μ_1 are respectively mean vector before and after the point τ and $f()$ is the multivariate normal distribution's probability density function. If $k < \tau$, means no shift has occurred in

the process, and the likelihood function for k is as below:

$$L_{\infty, k}(\mu_0) = \prod_{i=1}^k f(X_i | \mu_0, \Sigma_0) \quad (8)$$

Then the test statistic is

$$R_k = \frac{\log L_{\theta, k}(\mu_0, \mu_1)}{\log L_{\infty, k}(\mu_0)} = \max_{0 \leq \theta < k} \frac{k-\theta}{2} (\hat{\mu}_{1, \theta, k} - \mu_0)' \Sigma_0^{-1} (\hat{\mu}_{1, \theta, k} - \mu_0) \quad (9)$$

Where the maximum likelihood estimator (MLE) of μ_1 is $\hat{\mu}_{1, \tau, k} = \frac{\sum_{i=\tau+1}^k X_i}{k-\tau}$

This chart signals at time k if $R_k \geq h_{GLR}$, where h_{GLR} is the control limit determined via simulations based on a specific in-control performance.

In this research, spatiotemporal monitoring of electricity consumption using the $T^{\wedge 2}$ and GLR residual charts is performed in phase I. In statistical process control, understanding the process and evaluating its stability are the main objectives of Phase I. Phase I analysis is typically an iterative process. The control limits that are initially obtained are considered experimental limits and are revised repeatedly to ensure that the process is under control. When all the statistics of the charts are within the control limit, and there isn't a systematic pattern, we can say that the process is under control. On the contrary, the process is considered to be out-of-control if at least one statistic gets out of control limits. All out-of-control points are investigated, and if any assignable causes are detected, at first, the corresponding times (or observation or data) are saved for further investigation and then removed from the analysis. Then, based on the remaining data, the mean vector and covariance matrix, are re-estimated, the control limits are re-calculated, and the procedure is repeated until all chart statistics are within control limits and there are no assignable causes in the process or the number of observations is at least 2. Therefore, by using the process of identifying, rooting, removing and saving changes time repeatedly until reaching the in-controlled situation, the changes in electricity consumption are identified using the proposed charts.

The advantages of using multivariate $T^{\wedge 2}$ and GLR residual control charts for monitoring autocorrelated data include:

- 1- Improved sensitivity: By incorporating the autocorrelation structure, these control charts can detect subtle shifts in the mean vector and covariance structure, which may not be adequately captured by conventional control charts.
- 2- Better interpretation: The use of residuals allows for a more direct interpretation of deviations from the fitted model, providing insights into the specific nature and patterns of the observed abnormalities.
- 3- Timely detection: By monitoring the residuals in real-time, these control charts enable prompt detection of out-of-control conditions, facilitating timely corrective actions and intervention.

Overall, the multivariate $T^{\wedge 2}$ and GLR residual control charts offer a powerful approach for monitoring autocorrelated data, including energy consumption data.

3. A REAL CASE STUDY

The western cities of Mazandaran province have been welcomed by a large number of foreign tourists and domestic travelers due to their privileged tourism opportunities, such as the sea, forests, and pristine green villages. According to the published

information by the West Mazandaran Regional Electricity Distribution Company, the population of this region is about 793,000. There are about 693,000 electricity subscribers, including household, commercial, industrial, agricultural, and transportation, of which about 574,000 of them are household subscribers, and is considered as the most prominent consumer of electricity in the west of Mazandaran province. Fifty-one percent of household subscribers are the floating population, which plays a significant role in increasing electricity consumption in this region due to their presence in private villas and towns during holidays and also ignoring optimal consumption during peak usage hours.

Based on the expert's statements of West Mazandaran Regional Electricity Distribution Company, several factors are involved in the instability of the electricity network. One of the most important and influential factors in electricity consumption in the western cities of Mazandaran is non-native subscribers; that due to the instability of their covered population, the consumption of total subscribers cannot be accurately monitored, which also caused the taken actions for acculturation optimal electricity consumption have no effect on all subscribers. Another influential factor in increasing electricity consumption is rising temperatures and also the entrance of the north current, which moves from the sea to the mainland and brings moisture, causing muggy weather in coastal areas that eventually leads to increased use of cooling systems. In recent years, residents of different provinces of Iran have witnessed frequent blackouts of electricity due to the increased consumption of this energy carrier.

In addition to the mentioned factors, some factors such as outdated infrastructure, insufficient capacity, the lack of preventive maintenance, which are related to the technical instability of the electricity network, can also be involved in electricity consumption, which has been ignored due to the focus of the article on issues related to the consumption sector.

A. Data collection and analysis

In this subsection, the time series of electricity consumption in western cities of Mazandaran province, including eight cities (Ramsar, Abbasabad, Tonekabon, Kelardasht, Chaloos, Nowshahr, Noor, and Mahmoudabad), which are collected from the West Mazandaran Regional Electricity Distribution Company, is investigated over 154 days from March 21, 2019, to August 21, 2019.

Initially, the time series related to each city should be analyzed. The first step in time series analysis is data standardization which means rescaling the value distribution with a mean of 0 and a standard deviation of 1. The second stage is determining trend and seasonality components and then removing them to have a stationary process. Examinations indicate the existence of a trend component in the studied time series that can be eliminated by using the differentiation method. In the last stage, by investigating ACF and PACF plots, the existence of autocorrelation in time series data is confirmed. Accordingly, first, using the Box-Jenkins method, an appropriate ARIMA model is fitted to each time series based on their autocorrelation structure, and then the residuals are obtained, which are i.i.d and stable. The residuals of ARIMA models related to eight cities in each day are an 8-variate normal distribution represented by $X_k = [x_{1k}, x_{2k}, \dots, x_{8k}]$, $k = 1, 2, 3, \dots, 154$ where x_{ik} is the residual value obtained from the ARIMA model fitted to the first city at time k . these residuals are considered as input data for charts.

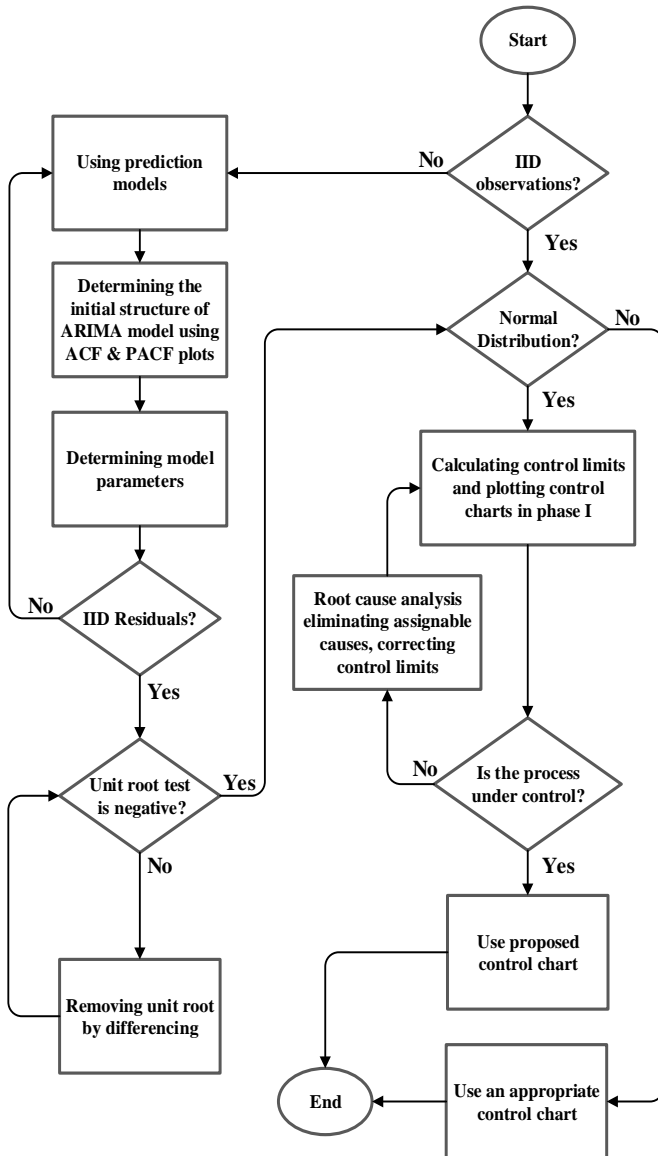


Fig. 1. Flowchart for residual-based control chart

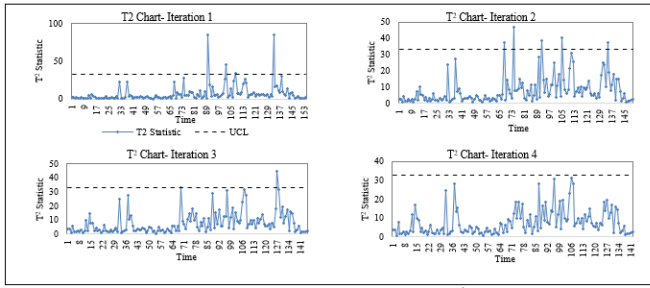


Fig. 2. Iteration results of the T^2 chart

Table 2. Moran's I result for in-control data of T^2 residual chart

Variable	Morans' I	E(I)	SE(I)	Z(I)	p-value
Electricity consumption	0.4201	-0.000291	0.0195	22.751	0

B. Results of T^2 residual chart

For the 154 observations under study with an 8-variate normal distribution, T^2 statistics and control limit are calculated according to in Figure 2, T2 statistics related to times 90, 102, 110, and 133 are out-of-control points. By removing these points and saving those as changes time in consumption, T2 statistics and control limit are re-calculated for the remaining 150 points. All iterations of the T2 chart, until reaching the in-control situation, are shown in Figure 2, Which can be concluded that after four iterations and detecting 11 points as changes time in consumption, the process will be in-control. The result of the Moran test for in-control data is shown in Table 2 Based on Table 2, the null hypothesis of no spatial correlation is rejected. In fact, the results indicate positive spatial autocorrelation in the intensity of electricity consumption in western cities of Mazandaran for in-control data. Figure 3 shows the geographical distribution of the average electricity consumption in the western cities of Mazandaran province in the in-control conditions. It can be seen that areas with higher consumption intensity have neighbors with similar characteristics, which shows a positive correlation in electricity consumption of cities and confirms Moran's result.

C. Results of GLR residual chart

GLR statistics are calculated for all observations under study and also using computer simulation and, considering the average sequence length (ARL) equal to the specified value of 200, the control limit is obtained. Similar to the results of the T2 chart, the results of the total iteration of the GLR chart are presented in Figure 5. It can be seen that after six iterations and detecting 20 points as changes time, the process will be in-control. The results of the Moran's I test for in-control data are shown in Table 3.

The results of Table 3 and also Figure 4, show a positive correlation in the intensity of electricity consumption in these cities in an in-control condition.

D. A Comparative assessment

One of the conventional methods of literature review that have been used for monitoring energy consumption is the univariate CUSUM chart. This chart is used for detecting the deviation of the observed values obtained from the samples with the target

Table 3. Moran's I result for in-control data of GLR residual chart

Variable	Morans' I	E(I)	SE(I)	Z(I)	p-value
Electricity consumption	0.4372	-0.0032	0.0203	24.131	0

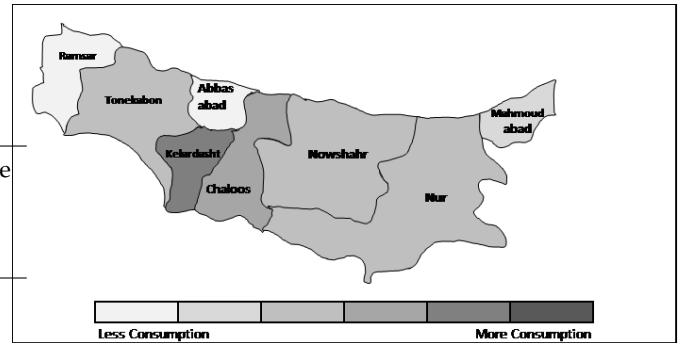


Fig. 3. Geographical distribution of the average electricity consumption in the western cities of Mazandaran province for in-control data of T^2 residual chart

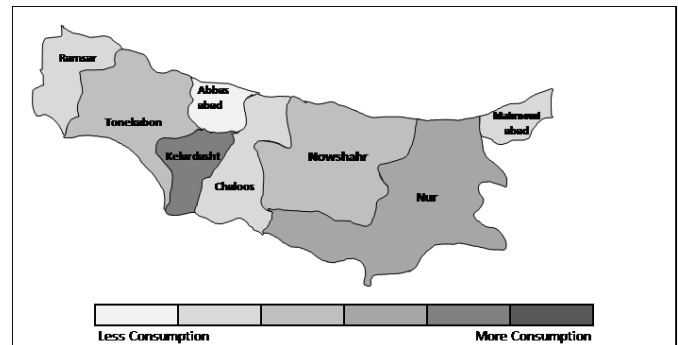


Fig. 4. Geographical distribution of the average electricity

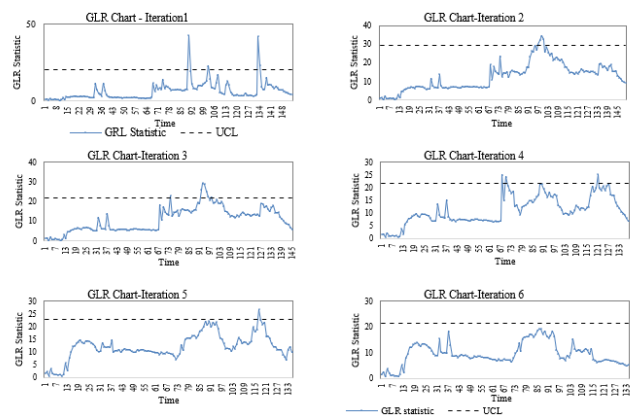


Fig. 5. Iteration results of the GLR chart

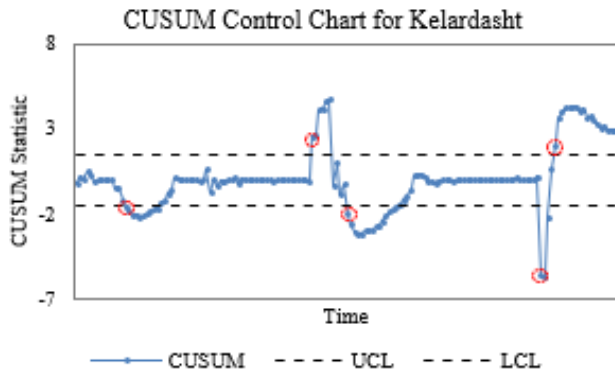


Fig. 6. The result CUSUM chart in Kelardasht

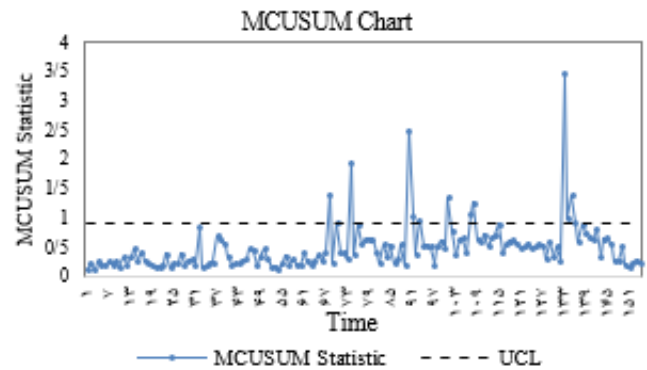


Fig. 7. The result of MCUSUM chart

value by plotting the cumulative sum of deviations.

The CUSUM chart was first introduced by Page [34], who defined CUSUM statistic as $C_i^+ = \max(0, x_i - (\mu_0 + k) + C_{i-1}^+)$ and $C_i^- = \max(0, -x_i + (\mu_0 - k) + C_{i-1}^-)$. Where X_i is the observed quality characteristic, μ_0 is the target value, k is the reference value, C^+ and C^- , are upper and lower CUSUM statistics, which are initially set to zero. Control limit h is determined by specific in-control ARL. If C^+ and C^- arises h , the related time is considered as a change point.

As mentioned in the literature review, Stuart et al. [5], considered the time series model related to electricity consumption data in an American school and, using a CUSUM chart, monitored the residuals of the determined model. And in another study, Puranik [6], has monitored electrical energy consumption in melting furnaces of foundry using the CUSUM chart. In this chart, in the situation of an existing out-of-control trend, only the first out-of-control point in the trend is considered as a change point.

In order to have a comparative assessment of T2 and GLR residual charts with CUSUM, we first monitored the residuals of fitted ARIMA models related to each city with CUSUM independently.

All results of CUSUM are shown in Figure. A in the appendix. Based on the analysis related to the time and location of the identified change points in GLR and T^2 , which are shown in Table 5 in detail, the number of detected change points in GLR, T^2 , and CUSUM in each city is briefly reported in Table 4. (For more detail, see Table A in the Appendix). As can be seen in Table 4, for Kalardasht, GLR detected 18 points as change time, whereas T^2 detected 10 points, all of which were detected by GLR. CUSUM chart for Kelardasht in Figure 6, indicated 5 points as a changes time, whereas just 2 points related to [68,133] are identified by both GLR and T^2 , and 3 other points at the time [15,78,137] were detected by none of them. By observing the results from other cities in Table 4, it can be seen that CUSUM has identified extra points as change, compared to the GLR and T^2 Chart.

To evaluate and check the accuracy of the detected changes of CUSUM, we used the MCUSUM chart, which is a multivariate extension of CUSUM and is a conventional multivariate control chart in SPC context, and relied on its results, which is shown in Figure 7. The result of MCUSUM showed, 11 change is occurred in time [68, 74, 90, 91, 93, 101, 107, 108, 133, 134, 135]. As shown in Table 4 for Tonekabon City, CUSUM detected 6 points related to [102,103,105,138,139,141] as changes time, in which these points are in-control points in MCUSUM.

By comparing the results of the CUSUM with the proposed charts through the MCUSUM chart, it can be said that due to the existence of temporal and spatial correlation in the electricity consumption data in different regions and the inability of the CUSUM chart in considering this feature, CUSUM considered some point as an out-of-control point whereas in MCUSUM they are considered as in-control point and conversely. So the CUSUM chart doesn't have the required efficiency and ability and is unable to correctly detect changes which may lead to providing wrong information about the process.

4. EVALUATING THE PERFORMANCE OF THE RESIDUAL T^2 AND GLR CHARTS

In this section, the performance of the proposed charts in detecting changes in electricity consumption is evaluated. For this purpose, based on the statements of electricity experts, the actual reasons for the changes in consumption during the period are identified, along with the out-of-control points and the detected locations of changes in the T^2 and GLR residual charts, presented in Table 5. The second and third columns of Table 5 are related to the change times identified by GLR and T^2 residual charts. The fourth column is T^2 decomposition results, and the fifth column is the graphs of the estimated mean vector in out-of-control points against the in-control mean vector, which respectively indicated the location of changes in T^2 and GLR residual charts. The reasons for actual changes in electricity consumption are given in the last column.

In the T^2 decomposition method, which determines each city's share in out-of-control points, the cities with a significant share are considered locations of change. In the GLR method, as proposed in [35], by plotting the estimated mean vector for out-of-control points against the in-control mean vector, the cities whose mean values have a difference from their in-control mean values are considered as the locations of changes.

The results of Table 5 show that the T^2 residual chart generally detected 11 out-of-control points as change times in consumption, while the GLR residual chart, in addition to all detected change times of the T^2 residual chart, and was able to detect 7 other points as change times in consumption. For example, in row 13, on August 1, in which a change in consumption was occurred because of rising temperatures and humidity, just the GLR chart was able to detect this change time.

In detecting location change in consumption, for example, in row 2, on May 29, which was detected by both charts as a change time, the T^2 decomposition method identified Kelardasht with

Table 4. number of change's detected in each city

Chart	Kelardasht	Ramsar	Chaloos	Nowshahr	Abbasbad	Nur	Mahmood abad	Tonekabon
GLR	18	9	2	1	1	0	0	0
T^2	10	3	2	1	1	0	0	0
CUSUM	5	8	5	2	3	4	4	6

a significant value of 30.468 as the location of change. In the GLR method, the plotted graph of estimated and in-control mean vectors shows that Kelardasht has the most significant difference compared to its in-control value and is considered as a location of the change in this method. In row 11, on July 6, that change occurs because of rising temperature, T^2 decomposition method detected Nowshahr and Chaloos as the locations of change, whereas the GLR graph indicated that 5 cities, including Nowshahr, Chaloos, Kelardasht, Mahmoudabad, and Nur have changes in their consumption in compared to normal consumption in which Nowshahr and Kalardasht with the most significant change in consumption are considered as locations of change.

In row 10, on July 5, based on the statement of electricity experts, a change occurred because of the Holiday and the entrance of a floating population. T^2 decomposition method showed that Chaloos, Kelardasht, and Ramsar had the most significant share of change while GLR detected 2 of these 3 locations including Kelardasht and Ramsar as locations with high consumption whereas it can be seen that all other cities have changed compared to their normal consumption.

By evaluating the results and comparing the identified changes time with the actual time of changes, and based on the statements of electricity experts, it can be stated the performance of the GLR chart is better than the T^2 chart in detecting times of change in consumption. And also, it can be said that, in general, both methods have almost the same performance in detecting the location of changes, whereas in the GLR method, in addition to detecting high-consumption locations, the locations that have changes in their consumption in compared to the normal situation, are recognizable. Another advantage of the GLR chart is that the estimations of the change time and out-of-control mean vector are available after calculating the GLR statistic. This feature makes it a favorable option for practitioners. Therefore, it can be said GLR residual chart has higher diagnostic power than T^2 residual chart, and also, in spatiotemporal monitoring of energy consumption, which requires high accuracy and sensitivity, using a GLR residual chart is recommended.

5. CONCLUSION

In this article, a spatiotemporal framework based on control charts was proposed for monitoring electricity consumption in the western cities of Mazandaran province, North of Iran. Due to the autocorrelation of spatial consumption data, a model-free monitoring approach was proposed for control charts to reduce the impact of autocorrelation on chart performance. In this approach, by using the box and Jenkins method, appropriate ARIMA models based on the autocorrelation structure of time series data were presented, and the independent residuals were obtained and monitored by proposed T^2 and GLR residual-based control charts. The performance of the proposed charts in identifying the actual time and location of changes was

evaluated. Results indicated a higher sensitivity and greater diagnostic power of the GLR chart compared to the T^2 chart. Therefore, in spatiotemporal monitoring of energy consumption which requires high accuracy and sensitivity, using a GLR residual chart is recommended. Spatiotemporal monitoring of energy carriers based on Panel-VAR models and nonparametric spatial regression models such as the Kriging method are interesting subjects for future research.

REFERENCES

1. E. Rizzo, F. Cousin, R. Lucca, and S. Lautenschlager, "Autonomous metering system for monitoring water consumption," *AQUA—Water Infrastructure, Ecosystems and Society*, vol. 70, no. 6, pp. 797–810, 2021.
2. K. L. Hameed and N. H. Barnouti, "Electricity monitoring and controlling iot smart system," in *2019 International Engineering Conference (IEC)*, pp. 182–187, IEEE, 2019.
3. M. Zini and C. Carcasci, "Machine learning-based monitoring method for the electricity consumption of a healthcare facility in italy," *Energy*, vol. 262, p. 125576, 2023.
4. J. Melendez, L. Burgas, F. Gamero, J. Colomer, and S. Herraiz, "Fault detection and diagnosis web service module for energy monitoring in buildings," *IFAC-PapersOnLine*, vol. 51, no. 10, pp. 15–19, 2018.
5. G. Stuart, P. Fleming, V. Ferreira, and P. Harris, "Rapid analysis of time series data to identify changes in electricity consumption patterns in uk secondary schools," *Building and Environment*, vol. 42, no. 4, pp. 1568–1580, 2007.
6. V. S. Puranik, "Cusum quality control chart for monitoring energy use performance," in *2007 IEEE International Conference on Industrial Engineering and Engineering Management*, pp. 1231–1235, IEEE, 2007.
7. L. Braga, A. Braga, and C. Braga, "On the characterization and monitoring of building energy demand using statistical process control methodologies," *Energy and Buildings*, vol. 65, pp. 205–219, 2013.
8. M. Shamsuzzaman, S. Haridy, I. Alsayouf, and A. Rahim, "Design of economic x chart for monitoring electric power loss through transmission and distribution system," *Total Quality Management & Business Excellence*, vol. 31, no. 5-6, pp. 503–523, 2020.
9. M. Shamsuzzaman, A. Shamsuzzoha, A. Maged, S. Haridy, H. Bashir, and A. Karim, "Effective monitoring of carbon emissions from industrial sector using statistical process control," *Applied Energy*, vol. 300, p. 117352, 2021.
10. S. Houidi, F. Auger, H. B. A. Sethom, D. Fourer, and L. Miègeville, "Multivariate event detection methods for non-intrusive load monitoring in smart homes and residential buildings," *Energy and Buildings*, vol. 208, p. 109624, 2020.
11. M. Faisal, R. F. Zafar, N. Abbas, M. Riaz, and T. Mahmood, "A modified cusum control chart for monitoring industrial processes," *Quality and Reliability Engineering International*, vol. 34, no. 6, pp. 1045–1058, 2018.
12. A.-M. Golmohammadi and S. K. Golestan, "Statistical process control for energy consumption monitoring in a cement factory iranian cement factory," *International Journal of Applied Optimization Studies*, vol. 1, no. 01, pp. 59–70, 2018.
13. D. C. Montgomery, *Introduction to statistical quality control*. John wiley & sons, 2019.

Table 5. Detected time and the location of changes in electricity consumption of Mazandaran province by T2 and GLR residual chart. (* indicates significance at the 0.05 level based on the one-sided upper critical value: 3.80. the blue line and red line are represented for the in-control mean vector and the estimated mean vector of out-of-control points in GLR chart.)

Row	GLR change time	T ² change time	Changes location in T ² (T ² decomposition)	Changes Location in GLR	Reason for change
1	May 27,2019	May 27,2019	Abbasabad 0.935 Chaloos 0.241 Kelardasht 30.468* Mahmoudabad 0.297 Nowshahr 0.816 Nur 0.164 Ramsar 0.000 Tonekabon 0.646	<p>The chart shows a red line representing the estimated mean vector and a blue dashed line for the in-control mean vector. A significant positive spike is observed at Kelardasht, reaching a value of approximately 2.8. Other locations remain near the zero line.</p>	Holiday and the entrance of a floating population
2	May 29,2019	May 29,2019	Abbasabad 0.935 Chaloos 0.241 Kelardasht 30.468* Mahmoudabad 0.297 Nowshahr 0.816 Nur 0.164 Ramsar 0.000 Tonekabon 0.646	<p>The chart shows a red line representing the estimated mean vector and a blue dashed line for the in-control mean vector. A significant positive spike is observed at Kelardasht, reaching a value of approximately 1.6. Other locations remain near the zero line.</p>	Rising temperatures
3	June 2,2019	June 2,2019	Abbasabad 0.935 Chaloos 0.241 Kelardasht 30.468* Mahmoudabad 0.297 Nowshahr 0.816 Nur 0.164 Ramsar 0.000 Tonekabon 0.646	<p>The chart shows a red line representing the estimated mean vector and a blue dashed line for the in-control mean vector. A significant negative spike is observed at Kelardasht, reaching a value of approximately -2.5. Other locations remain near the zero line.</p>	Between holidays and the entrance of a floating population
4	June 18,2019	June 18,2019	Abbasabad 0.935 Chaloos 0.241 Kelardasht 30.468* Mahmoudabad 0.297 Nowshahr 0.816 Nur 0.164 Ramsar 0.000 Tonekabon 0.646	<p>The chart shows a red line representing the estimated mean vector and a blue dashed line for the in-control mean vector. A significant negative spike is observed at Kelardasht (approx. -0.15) and a significant positive spike is observed at Ramsar (approx. 0.25). Other locations remain near the zero line.</p>	Entrance of the north stream and increasing humidity

Row	GLR change time	T ² change time	Changes location in T ² (T ² decomposition)	Changes Location in GLR	Reason for change
5	June 18,2019	-	-		Entrance of the north stream and increasing humidity
6	June 21, 2019	June 21, 2019	Abbasabad 0.935 Chalooos 0.241 Kelardasht 30.468* Mahmoudabad 0.297 Nowshahr 0.816 Nur 0.164 Ramsar 0.000 Tonekabon 0.646		Rising temperatures, holiday and the entrance of a floating population
7	June 24, 2019	June 2,2019	-		Rising temperatures
8	June 26,2019	June 18,2019	-		Rising temperatures (the hottest day of the year)

Row	GLR change time	T ² change time	Changes location in T ² (T ² decomposition)	Changes Location in GLR	Reason for change
9	June 27-29,2019	-	-		long weekend and the entrance of a floating population
10	July 5, 2019	July 5, 2019	Abbasabad 0.371 Chalooos 25.262* Kelardasht 4.737* Mahmoudabad 2.946 Nowshahr 2.09 Nur 1.022 Ramsar 4.558* Tonekabon 2.554		Holiday and the entrance of a floating population
11	July 6, 2019	July 6, 2019	Abbasabad 0.341 Chalooos 7.477* Kelardasht 0.000 Mahmoudabad 0.267 Nowshahr 19.540* Nur 2.507 Ramsar 0.012 Tonekabon 0.176		Rising temperatures
12	July 31, 2019	July 31, 2019	Abbasabad 1.329 Chalooos 1.933 Kelardasht 29.494* Mahmoudabad 0.943 Nowshahr 1.000 Nur 0.540 Ramsar 0.050 Tonekabon 0.068		Rising temperatures

Row	GLR change time	T ² change time	Changes location in T ² (T ² decomposition)	Changes Location in GLR	Reason for change
13	August 1,2019	-	-		Rising temperatures and humidity
14	August 2,2019	August 2,2019	Abbasabad 4.059* Chaloo 0.147 Kelardasht 31.738* Mahmoudabad 0.328 Nowshahr 0.000 Nur 1.016 Ramsar 3.384 Tonekabon 1.912		Rising temperatures and humidity, holiday and the entrance of a floating population
15	August 3,2019	August 3,2019	Abbasabad 0.006 Chaloo 3.185 Kelardasht 32.915* Mahmoudabad 0.006 Nowshahr 3.086 Nur 0.073 Ramsar 0.241 Tonekabon 0.003		Rising temperatures and humidity
16	August 5,2019	August 5,2019	Abbasabad 0.000 Chaloo 1.908 Kelardasht 6.337* Mahmoudabad 0.929 Nowshahr 0.963 Nur 1.104 Ramsar 0.864 Tonekabon 0.784		Rising temperatures and humidity, holiday and the entrance of a floating population

Row	GLR change time	T^2 change time	Changes location in T^2 (T^2 decomposition)	Changes Location in GLR	Reason for change
17	August 8,2019	-	-		holiday and the entrance of a floating population
18	August 9,2019	-	-		holiday and the entrance of a floating population

14. W. Jiang, S. W. Han, K.-L. Tsui, and W. H. Woodall, "Spatiotemporal surveillance methods in the presence of spatial correlation," *Statistics in Medicine*, vol. 30, no. 5, pp. 569–583, 2011.

15. D. Wang, F. Li, and K. Liu, "Modeling and monitoring of a multivariate spatio-temporal network system," *IISE Transactions*, vol. 55, no. 4, pp. 331–347, 2023.

16. J. Derenski, E. Porse, H. Gustafson, D. Cheng, and S. Pincetl, "Spatial and temporal analysis of energy use data in los angeles public schools," *Energy Efficiency*, vol. 11, pp. 485–497, 2018.

17. F. M. Megahed, L. J. Wells, J. A. Camelio, and W. H. Woodall, "A spatiotemporal method for the monitoring of image data," *Quality and Reliability Engineering International*, vol. 28, no. 8, pp. 967–980, 2012.

18. Z. He, L. Zuo, M. Zhang, and F. M. Megahed, "An image-based multivariate generalized likelihood ratio control chart for detecting and diagnosing multiple faults in manufactured products," *International Journal of Production Research*, vol. 54, no. 6, pp. 1771–1784, 2016.

19. M. Koosha, R. Noorossana, and F. Megahed, "Statistical process monitoring via image data using wavelets," *Quality and Reliability Engineering International*, vol. 33, no. 8, pp. 2059–2073, 2017.

20. L. Zuo, Z. He, and M. Zhang, "An ewma and region growing based control chart for monitoring image data," *Quality Technology & Quantitative Management*, vol. 17, no. 4, pp. 470–485, 2020.

21. B. M. Colosimo and M. Grasso, "Spatially weighted pca for monitoring video image data with application to additive manufacturing," *Journal of Quality Technology*, vol. 50, no. 4, pp. 391–417, 2018.

22. R. Noorossana and S. J. M. Vaghefi, "Effect of autocorrelation on performance of the mcusum control chart," *Quality and Reliability Engineering International*, vol. 22, no. 2, pp. 191–197, 2006.

23. S.-H. Sheu and S.-L. Lu, "Monitoring autocorrelated process mean and variance using a gwma chart based on residuals," *Asia-Pacific Journal of Operational Research*, vol. 25, no. 06, pp. 781–792, 2008.

24. H. Khusna, M. Mashuri, Suhartono, D. D. Prastyo, M. H. Lee, and M. Ahsan, "Residual-based maximum mcusum control chart for joint monitoring the mean and variability of multivariate autocorrelated processes," *Production & Manufacturing Research*, vol. 7, no. 1, pp. 364–394, 2019.

25. B. Žmuk, "Capabilities of statistical residual-based control charts in short-and long-term stock trading.," *Our Economy (Nase Gospodarstvo)*, vol. 62, no. 1, 2016.

26. G. C. Runger and T. R. Willemain, "Model-based and model-free control of autocorrelated processes," *Journal of Quality Technology*, vol. 27, no. 4, pp. 283–292, 1995.

27. G. E. Box, G. M. Jenkins, G. C. Reinsel, and G. M. Ljung, *Time series analysis: forecasting and control*. John Wiley & Sons, 2015.

28. R. Noorossana, M. Eyvazian, A. Amiri, and M. A. Mahmoud, "Statistical monitoring of multivariate multiple linear regression profiles in phase i with calibration application," *Quality and Reliability Engineering International*, vol. 26, no. 3, pp. 291–303, 2010.

29. W. R. Tobler, "A computer movie simulating urban growth in the detroit region," *Economic geography*, vol. 46, no. sup1, pp. 234–240, 1970.

30. P. A. Moran, "Notes on continuous stochastic phenomena," *Biometrika*, vol. 37, no. 1/2, pp. 17–23, 1950.

31. H. Hotelling, "Multivariate quality control-illustrated by the air testing of sample bombsights," *Techniques of statistical analysis*, 1947.

32. D. S. Holmes and A. E. Mergen, "Improving the performance of the t2 control chart," *Quality Engineering*, vol. 5, no. 4, pp. 619–625, 1993.

33. R. L. Mason, N. D. Tracy, and J. C. Young, "Decomposition of t2 for multivariate control chart interpretation," *Journal of quality technology*, vol. 27, no. 2, pp. 99–108, 1995.

34. E. Page, "Cumulative sum charts," *Technometrics*, vol. 3, no. 1, pp. 1–9, 1961.

35. S. Wang and M. R. Reynolds Jr, "A glr control chart for monitoring the mean vector of a multivariate normal process," *Journal of Quality Technology*, vol. 45, no. 1, pp. 18–33, 2013.

APPENDIX

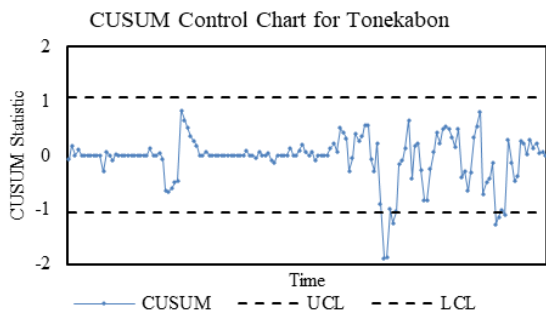
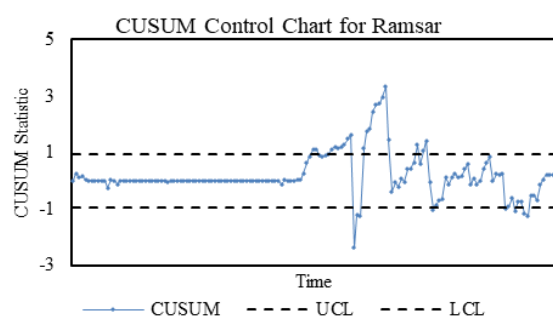
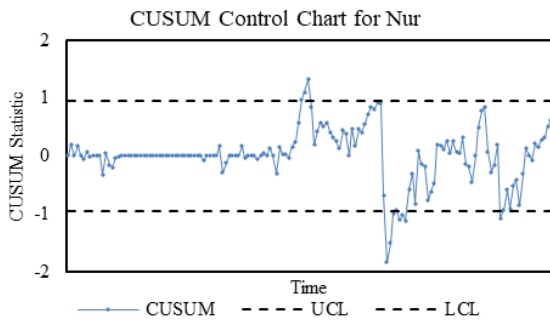
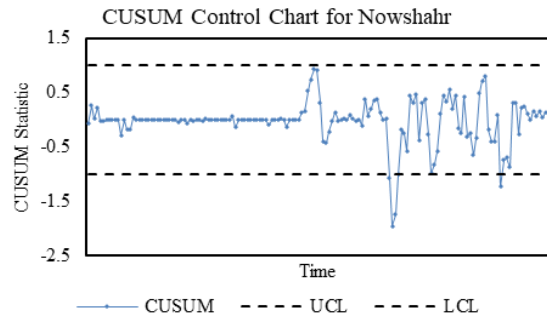
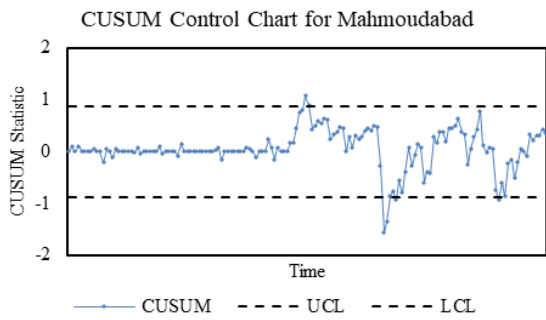
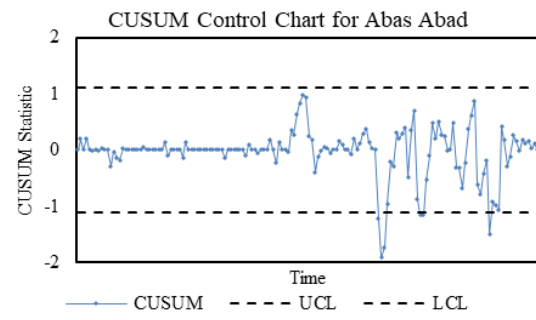
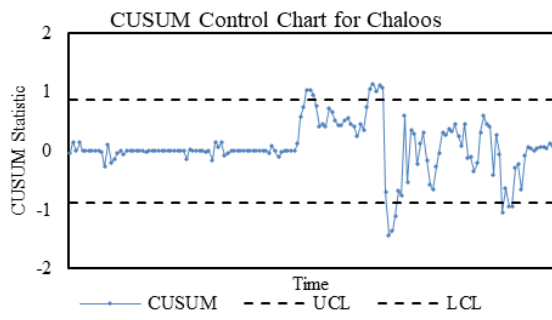


Fig A. CUSUM chart result for all cities

Table A. Detail of detected changes time by GLR, T2 and CUSUM chart's for each city independently

Change Time	Kelardasht			Ramsar			Chaloos			Nowshahr			Abbasabad			Nur			Mahmoudabad			Tonekabon		
	GLR	T2	CUSUM	GLR	T2	CUSUM	GLR	T2	CUSUM	GLR	T2	CUSUM	GLR	T2	CUSUM	GLR	T2	CUSUM	GLR	T2	CUSUM	GLR	T2	CUSUM
15			*																					
68	*	*	*																					
70	*	*																						
74	*	*																						
75																		*						
76									*															
77						*														*				
78			*																					
82						*																		
90	*	*		*	*																			
91				*																				
93	*	*		*	*																			
96	*			*					*															
98	*			*																				
99	*			*																				
100	*			*																				
101	*			*							*			*										
102									*							*			*					*
103																								*
105																								*
106																*			*					
107	*	*		*	*		*	*																
108							*	*		*	*													
110						*																		
112						*																		
115						*								*										
133	*	*	*																					
134	*																							
135	*	*											*	*										
136	*	*																						
137			*																					
138	*	*				*			*		*			*		*		*		*			*	*
139																		*					*	*
140									*															
141	*					*																		*
142	*																							
144						*																		
Temporal Change	18	10	5	9	3	8	2	2	5	1	1	2	1	1	3	0	0	4	0	0	4	0	0	6